

The central cusps in dark matter halos: fact or fiction?

A.N. Baushev¹ and S.V. Pilipenko²

¹ Bogoliubov Laboratory of Theoretical Physics, Joint Institute for Nuclear Research, 141980 Dubna, Moscow Region, Russia

² Astro Space Center of P.N.Lebedev Physical Institute, Russian Academy of Sciences, Profsoyuznaja 84/32, 117997 Moscow, Russia

ABSTRACT

We investigate the reliability of standard N-body simulations by modelling of the well-known Hernquist halo with the help of GADGET-2 code (which uses the tree algorithm to calculate the gravitational force) and ph4 code (which uses the direct summation). Comparing the results, we find that the core formation in the halo center (which is conventionally considered as the first sign of numerical effects, to be specific, of the collisional relaxation) has nothing to do with the collisional relaxation, being defined by the properties of the tree algorithm. This result casts doubts on the universally adopted criteria of the simulation reliability in the halo center. Though we use a halo model, which is theoretically proved to be stationary and stable, a sort of numerical 'violent relaxation' occurs. Its properties suggest that this effect is highly likely responsible for the central cusp formation in cosmological modelling of the large-scale structure, and then the 'core-cusp problem' is no more than a technical problem of N-body simulations.

Key words. dwarf galaxies, dark matter theory, galaxy evolution, rotation curves of galaxies

1. Introduction

N-body simulations of the origin of present-day cosmic objects from initial small perturbations is not only popular, but almost inevitable method of studying the large-scale structure formation in the Universe: the task is highly nonlinear and complex, which makes numerical methods to be the only direct approach to the problem. Simulating the structure formation under various cosmological assumptions and comparing the results with observations one may check the applicability of the cosmological models. Probably, the strongest result that has been derived from N-body cosmological simulations is the core-cusp problem (see (de Blok 2010) for a review). Simulations of the Λ CDM Universe always predict that dark matter (hereafter DM) halos have either a high density core or a very steep density profile in the center (Gao et al. 2008; Dutton & Macciò 2014) (for the sake of simplicity, this dense central region is named 'a cusp', despite of its shape). However, abundant observations of galaxies favor a respectively large and low-density cores in their central regions: the dark matter mass there is much lower than the cusp should contain (Chemin et al. 2011; Walker & Peñarrubia 2011). This discrepancy is known for many years at the galaxy scale, but some recent observations disfavor cusps in the galaxy clusters as well (Harvey et al. 2017).

The core-cusp problem may indicate that the cold dark matter model is incorrect. However, only irreproachably reliable estimations of the simulation accuracy and convergence may permit to make so strong physical conclusions. N-body simulations may suffer from several numerical effects; we mention only the major ones.

Collisional relaxation of the test particles is an unphysical effect, if one models dark matter, which is believed to be collisionless (Binney & Knebe 2002). In the case of a spherical halo, the process may be characterized by the relaxation time

(Binney & Tremaine 2008, eqn. 1.32)

$$\tau_r = \frac{N(r)}{8 \ln \Lambda} \cdot \tau_d \quad (1)$$

where $\ln \Lambda = \ln(b_{max}/b_{min})$ is the Coulomb logarithm (b_{max} and b_{min} are the characteristic maximum and minimum values of the impact parameter), $N(r)$ is the number of test particles inside radius r , $\tau_d = (4\pi G \bar{\rho}(r)/3)^{-1/2}$ is the characteristic dynamical time of the system at radius r , $\bar{\rho}(r)$ is the average density inside r . It is noteworthy that the potential softening used in the N-body simulations allows to avoid close collisions of the particles, but scarcely affects the collisional relaxation time: b_{min} is of the order of the softening radius, but τ_r depends on it only logarithmically. We will use $\ln \Lambda = \ln(3r_s/\epsilon)$, where ϵ is the softening radius, like in (Baushev et al. 2017).

The softening of the gravitational potential is an another source of computation errors. If ϵ is too small, close two-body collisions on large angles occur. If the value of ϵ is too large, it smooths away the high density peaks and introduces a bias in the force computation. The optimal choice of softening has been a subject of many studies, see, e.g. (Merritt 1996; Athanassoula et al. 2000; Knebe et al. 2000; Dehnen 2001; Zhan 2006).

The third potential source of undesirable numerical effects is the gravitational interaction computations. The direct summation is exact, but very resource-intensive algorithm, since it requires to calculate $N - 1$ partial forces per particle in a system containing N particles. It means that we need $\sim N^2$ partial force calculations for all the system. Many N-body codes use a hierarchical tree algorithm (Barnes & Hut 1986; Hernquist & Katz 1989), which is significantly more economical. The idea of the method is to group distant particles into larger cells and calculate their gravity as a single multipole force. A recursive subdivision of space is used to achieve the required spatial adaptivity. For instance, the algorithm of the GADGET code (Springel 2005) divides the space in cubic cells. Each cell is repeatedly subdivided into eight daughter ones until the ratio between the distance to

Send offprint requests to: baushev@gmail.com

the cell and the size of the cell exceeds the parameter specified by the user. The GADGET code that we consider in this paper splits the cells until the following cell-opening criterion is satisfied

$$\frac{GM_{\text{cell}}}{r^2} \left(\frac{l}{r}\right)^2 \leq f_{\text{acc}} |\mathbf{a}|, \quad (2)$$

where M_{cell} and l are the cell mass and extension, r is the distance to the cell, $|\mathbf{a}|$ is the value of the total acceleration obtained in the last timestep, and f_{acc} is a tolerance parameter (see (Springel 2005, equation (18)), where f_{acc} is denoted by α). The interaction with the closest particles is calculated by the direct summation. Requiring only $O(N \ln N)$ partial force calculations for all the system, the tree algorithm is, generally speaking, much faster than the direct summation. The price to pay is that the result represents only an approximation to the true force.

Finally, figure 4 in (Springel 2005) gives a highly visual illustration of significant numerical phenomena appearing during the temporal integration of particle orbits. Thus, several unphysical effects inevitably occur in the simulations, and their correct estimation is necessary for an appropriate interpretation of simulation results.

However, the present state-of-art of N-body simulation tests (especially, of the DM behavior) can hardly be named adequate. The commonly-used criterion of the convergence of N-body simulations in the halo center is solely the density profile stability (Power et al. 2003): these simulations show that the central cusp (close to $\rho \propto r^{-1}$) is formed quite rapidly ($t < \tau_r$). The shape of the cusp and its stability is insensitive to the simulation parameters (see, e.g. (Hayashi et al. 2003)). Considering the temporal dependence of the overdensity inside various radii r from the halo center (i.e., the ratio of the average density inside radius r from the halo center to the average universe density), (Power et al. 2003) find that a core forms in the center no earlier, than $t(r) = 1.7\tau_r(r)$. We will denote this time by $\tau_p(r) = 1.7\tau_r(r)$. The authors assume that cusp universality and stability implies the negligibility of numerical effects, and the core formation is the first sign of the collisional relaxation. Therefore, (Power et al. 2003) suggest that N-body simulation results are trustable until $t(r) = 1.7\tau_r(r)$. The reasons why the collision influence can be neglected at almost two relaxation times are not quite clear. Moreover, (Hayashi et al. 2003) and (Klypin et al. 2013) report that the cusp is stable much longer, probably, up to tens of relaxation times.

The weak point of this reasoning is that the profile stability by itself does not guarantee the absence of the collisional influence. Indeed, if the collisions are already significant, but the particles mainly scatter on small angles in the collisions (the latter is true for N-body simulations), the system can be described by the Fokker-Planck equation. This equation may have a stationary solution (Evans & Collett 1997; Baushev 2015; Baushev & Barkov 2018), and if it is stable, it works as a sort of attractor: the collisions tend to transform an initial distribution into the stationary one. Then the attractor profile should survive for much longer than τ_r , since the Fokker-Planck diffusion is self-compensated in this case. The profile corresponding to the stationary solution should also be quite universal, since its shape is defined by the the Fokker-Planck coefficients (i.e., by the potential of the particle interaction) that are similar for various N-body packages. However, the profile universality and stability have nothing to do with the simulation veracity: it is already created by test particle collisions, that is, by a purely numerical effect. It seems to be no coincidence that the Fokker-Planck equation really has a stationary solution that is similar

to $\rho \propto r^{-1}$ in the halo center (Evans & Collett 1997; Baushev 2015) and close to the Einasto profile with $n \sim 6$ at $r \sim 10^{-1}r_s$ (Baushev & Barkov 2018).

Another way to test N-body simulations is to model an analytical solution and compare the results with theoretical predictions. Simulations of an isolated spherically symmetric halo allow to go beyond the density profile stability and consider the full array of dynamical parameters of the particles. (Baushev et al. 2017) modelled a Hernquist halo and found that all integrals of motion characterizing individual particles experience strong unphysical variations along the whole halo, revealing an effective interaction between the test bodies. Moreover, the simulations show that the cusp stability is really provided with the particle collisions, as we described in the previous paragraph: intense upward and downward Fokker-Planck streams of particles in the cusp region occur, and the cusp is stable because they compensate each other. This result suggests that the cusps in cosmological N-body simulations may also be a consequence of numerical effects.

However, the paper (Baushev et al. 2017) has not answered to several important questions. Though significant unphysical effects were found, the immediate causes of them, as well as their dependence from the N-body code parameters, remained unclarified. The fact that the variations of the integrals of motion of individual particles were significant at very large radii, where the influence of the collisions and potential softening was certainly negligible, implied that the integral variations there are most likely due to the potential calculating algorithm. In order to clarify this point, we perform a new simulation of the Hernquist halo, following the way described in (Baushev et al. 2017). However, contrary to that work, we evolve the same initial conditions for the halo using the GADGET-2 code with various parameter settings. Besides, we follow the system evolution in a 4-th order Hermite code, which uses the direct summation algorithm to calculate the gravitation force, and thus is free from the tree algorithm drawbacks. Comparing the results, we may elucidate the cause of the unphysical effects and clarify their dependence from the code parameters.

In Sect. 2 we describe the codes we used and the simulation setup, in Sect. 3 we present the methods we use to treat the data, in Sect. 4, we present the results of the simulations and discuss them. Finally, in Sect. 5 we briefly summarize the obtained results.

2. Simulations

2.1. The simulation setup

We evolve the system using one of the most extensively employed in cosmological simulations SPH codes, GADGET-2 (Springel et al. 2001; Springel 2005)¹. We vary the cell-opening parameter f_{acc} to check the impact of the tree algorithm on the system evaluation. The lower the value of f_{acc} is, the more GADGET-2 resembles a direct summation algorithm with the second order accuracy of temporal integration. The default value of f_{acc} recommended by (Springel 2005) is $5 \cdot 10^{-3}$. So we use three values: $f_{\text{acc}} = 5 \cdot 10^{-5}$, $5 \cdot 10^{-4}$, and $5 \cdot 10^{-3}$. For comparison, we also use a 4-th order direct summation parallel Hermite code with individual particle time steps, which is a part of AMUSE suite (Portegies Zwart et al. 2009; van Elteren et al. 2014) and is called “ph4” inside it. Of course, the direct summation code is

¹ Actually, the dark matter part of the GADGET-3 code coincides with that of the GADGET-2. The codes differ only in the barionic matter part.

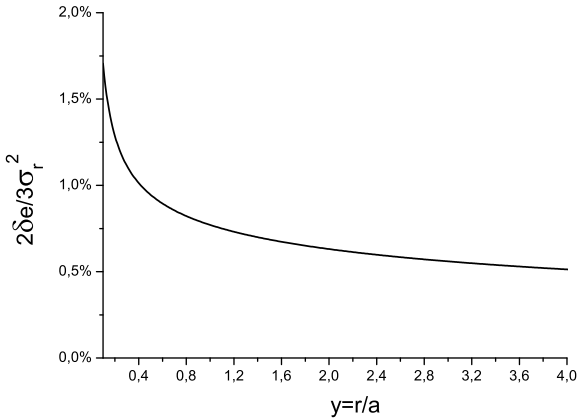


Fig. 1. The ratio of the perturbation energy of the clump particles δe (see eqn. 11) to the average kinetic energy of the particles $\bar{e}_k \approx 3\sigma_r^2/2$, as a function of radius.

much slower than the tree one. All ph4 simulations were run at the Lomonosov supercomputer of the Moscow State University computer center².

Thus, the GADGET-2 and ph4 codes have significantly different field calculation algorithms. However, they differ little in other calculation performance: both the codes utilize the leapfrog algorithm to calculate the test particle trajectories, and very similar gravitational softening to avoid close particle collisions. In ph4, the value of the softening radius ϵ gives the radius of a Plummer ‘sphere’, i.e. the gravitational potential of a point mass is calculated as $-Gm/\sqrt{r^2 + \epsilon^2}$. The GADGET-2 code uses the same value of the potential at zero radius $-Gm/\epsilon$ and represents the density distribution of a point mass by a spline kernel. Thus, despite of some difference in gravitational softening, the meaning of the softening parameter is the same for both codes. We ignore all the data inside $0.1a = 10$ pc (i.e., ~ 6 softening radii ϵ if $\epsilon = 1.7$ pc and $\sim 3\epsilon$ if $\epsilon = 3.4$ pc) from the halo center in order to avoid the influence of the potential softening on the cusp.

2.2. The Hernquist profile

The Hernquist profile has the shape

$$\rho_{ini}(r) = \frac{Ma}{2\pi r(r+a)^3}, \quad M_r(r) = M \frac{r^2}{(r+a)^2} \quad (3)$$

where M is the total halo mass, $M_r(r)$ is the halo mass inside radius r , a is the Hernquist radius, $r_s = a/2$ (Hernquist 1990). It is important that it behaves exactly as the NFW in the center. The specific angular momentum K_{circ} corresponding to a circular orbit of radius r is

$$K_{circ}(r) = \sqrt{GM} \frac{r^{3/2}}{(r+a)}. \quad (4)$$

We set $M = 10^9 M_\odot$, $a = 100$ pc, which roughly corresponds to the well-known dwarf satellite of the Milky Way, Draco, as it was before the tidal destruction (Łokas 2002). Since we use the standard N-body units (Hénon 1971), the results are independent on the choice of a and halo mass. However, it defines the time scale, and we choose the realistic values for illustrative purposes.

² <http://parallel.ru>

It is convenient to introduce the Hernquist time $\xi = \left(\frac{GM}{a^3}\right)^{-1/2}$ and the dimensionless radius $y \equiv r/a$. Then

$$\tau_d = \xi(y+1)\sqrt{y}; \quad \tau_r = \frac{N\xi}{8 \ln \Lambda} \frac{y^2 \sqrt{y}}{(y+1)}. \quad (5)$$

Here N is the total number of particles in the Hernquist halo.

In order to generate the initial conditions, we place randomly $N \sim 10^5$ test bodies of equal masses, in accordance with the analytically obtained space and velocity distributions, corresponding to the Hernquist profile (Hernquist 1990). Theoretically, the halo should be stable: not only the density profile, but even the energy and angular momentum components of each particle should be conserved. Any deviation from this behavior is a numerical effect. The relatively small number N of test particles comes from the slowness of the direct summation algorithm: simulations for $N = 10^6$ particles would last for too long. On the other hand, even recent and high-performance cosmological simulations contain only a few of halos with $\sim 10^6$ test particles (Dutton & Macciò 2014).

Our main simulation contains $N = 10^5$ particles. We choose the softening length $\epsilon = 0.5aN_a^{-1/3}$, where N_a is the number of particles inside radius a around the halo center. This value of the gravitational softening length ($\epsilon = 1.7$ pc in our case) is found to be optimal for the Hernquist profile (Dehnen 2001). Then the Coulomb logarithm is equal to $\ln \Lambda \approx 4.5$ for the halo under consideration, $\xi = 4.72 \cdot 10^6$ years, and

$$\tau_d = (y+1)\sqrt{y} \times 0.472 \cdot 10^6 \text{ years}; \quad \tau_r = \frac{2y^2 \sqrt{y}}{(y+1)} \times 1.36 \cdot 10^9 \text{ years}. \quad (6)$$

At $r = a$ $\tau_d = 2 \cdot \xi = 0.945 \cdot 10^6$ years, $\tau_r = 1.36 \cdot 10^9$ years. We consider this simulation as the main one, and it covers the maximum duration $2.85 \cdot 10^9$ years = 2.85 Gyr. Hereafter we always consider this simulation in these paper, unless the opposite is indicated. If the name of a simulation is not specified somewhere in the text, we mean this one.

To check the result reliability, we perform an auxiliary simulation with the same number of particles (10^5), but with the doubled softening length $\epsilon = 3.4$ pc. Moreover, we create the initial condition setting the random number generator independent from the first simulation, which gives us a possibility to estimate the importance of the Poisson noise (see below). Since we are short of calculational power, the simulation covers only $0.85 \cdot 10^9$ years = 0.85 Gyr. Every time when we use this auxiliary simulation, we specify it, so it may not lead to a misunderstanding.

We model an astrophysical stationary DM halo, which has a smooth and constant gravitational potential $\phi(r)$. Therefore, the specific energy $w = \phi(r) + v^2/2$ and the specific angular momentum \mathbf{K} of each particle should be conserved³. Instead of w , it is more convenient to use the apocenter distance of the particle r_0 (i.e. the maximum distance on which the particle can move off the center, which can be found from the implicit equation $w = \phi(r_0) + K^2/2r_0$). We analyze the behavior of K , K_x , K_y , K_z , and r_0 (r_0 is an integral of motion as an implicit function of the

³ Sometimes we will name ‘specific energy’ and ‘specific angular momentum’ simply by ‘energy’ and ‘angular momentum’. Since we never use real energies and angular momenta of the particles in this paper, it cannot lead to any misunderstanding.

integrals of motion w and K) of individual particles in our simulations. Any temporal variation of these values is necessarily a numerical effect.

2.3. Is the Poisson noise significant?

However, the numerical effects may be produced not only by N-body codes, but by inaccuracies of the initial conditions as well. The only significant source of errors in the initial conditions we use is the Poisson noise: since the particles are placed randomly, they may stochastically form clumps, and we should estimate the influence of this effect. Let us consider a Poisson clump of mass m occurred at a radius l (and dimensionless radius $y \equiv l/a$) from the halo center. The number of particles in the clump is $\sim Nm/M$, where N and M are the total mass and the number of particles in the halo. The standard deviation of this quantity is $\sim \sqrt{Nm/M}$, and the standard deviation of the clump mass is $\delta m \sim m \sqrt{M/(Nm)} = \sqrt{Mm/N}$.

Two questions should be discussed:

1. Will the clump grow?
2. What characteristic perturbations of the integrals of motion K_x, K_y, K_z , and r_0 may the Poisson noise produce?

The answer on the first one is certainly negative. First, let us suppose that the clump of radius r is gravitationally bound (we will see that it is not really so), but even then the clump will be destroyed by the tidal force of the main halo. Indeed, the characteristic size of many particle orbits in the clump of radius r is r . The tidal gravitational force from the main halo can be estimated as $\sim (GM(l)/l^2) \cdot (r/l)$ in the framework of the clump center. The work of the force on the particle orbit is $\sim r(GM(l)/l^2) \cdot (r/l)$. If it exceeds the binding energy of the particle $\sim Gm/r$, the particle can be teared out of the clump: $r(GM(l)/l^2) \cdot (r/l) > Gm/r$, or $(M(l)/l^3) > (m/r^3)$. This inequality may be rewritten as $\bar{\rho}(l) > \rho(l)$, where $\bar{\rho}(l)$ and $\rho(l)$ are the average halo density inside radius l and the halo density at radius l , respectively: the relative overdensity of the clump is small $\delta m/m \sim 1/\sqrt{N}$ and may be neglected. But the inequity $\bar{\rho}(l) > \rho(l)$ is always true, since the central region of the halo is denser. Thus, tidal perturbations exceed the binding energy of the Poisson clumps, and they are easily destroyed. This is a special case of a general regularity: a clump can be stable only if its density is significantly higher than the halo density (Baushev 2016).

Second, the Poisson clumps in our system cannot be gravitationally bound at all. Then $r \sim \sqrt[3]{3m/(4\pi\rho(l))}$, where we should substitute (3) instead of $\rho(y)$.

$$r \sim \sqrt[3]{\frac{3m}{4\pi\rho(l)}}, \quad (7)$$

where we should substitute (3) instead of $\rho(l)$. The standard deviation of particle energy δe produced by the clump is $\delta e = G\delta m/r$. We obtain:

$$\delta e \sim 0.8 \frac{GM}{a} N^{-1/2} \frac{(m/M)^{1/6}}{\sqrt[3]{y(y+1)}}. \quad (8)$$

As we can see, the Poisson noise depends on the clump mass rather weakly, only as $m^{1/6}$.

Deriving this equation, we supposed (equation 7) that the average density of the clump is equal to to the clump central density. This is apparently not true if $r \gg l$: then the clump center is

very close to the halo center, and $\rho(l)$ by far exceeds the average clump density. In fact, the average clump density cannot exceed

$$\min\left(\sqrt[3]{\frac{3M(l)}{4\pi l^3}}, \sqrt[3]{\frac{3M(r)}{4\pi r^3}}\right). \quad (9)$$

As a result, equation 8 for δe diverges as $\sqrt[3]{y}$ when $y \rightarrow 0$. In order to avoid this difficulty, we limit ourself by considering only the case when the halo center does not lie inside the clump, i.e., $r < l$. Then m by no means can exceed $M(l)$. With the help of equation (3) we obtain:

$$\frac{m}{M} < \frac{M(l)}{M} = \frac{y^2}{(y+1)^2}, \quad \text{i.e.} \quad \frac{(m/M)^{1/6}}{\sqrt[3]{y}} < (y+1)^{1/3} \quad (10)$$

With the help of this inequality, we obtain from (8)

$$\delta e \sim 0.8 \frac{GM}{a} N^{-1/2} (y+1)^{-4/3}. \quad (11)$$

The characteristic velocity of the particles in the clump is the particle velocity dispersion σ , corresponding to the Hernquist profile. Since the velocity distribution is isotropic, the velocity dispersions are equal in all three directions, i.e. the average squared velocity of the particles is $v^2 \sim 3\sigma^2$. The measure of the Poisson clump stability is the ratio $\alpha \equiv 2\delta e/v^2 = 2\delta e/3\sigma^2$. Calculation of σ_r^2 for the Hernquist profile is trivial, but rather cumbersome (Binney & Tremaine 2008, equation 4.35b).

Figure 1 shows the ratio $\alpha = \delta e/\bar{e}_k = 2\delta e/3\sigma_r^2$ (i.e., the ratio of the gravitational binding energy of the clump particles to the average kinetic energy of the particles) as a function of radius. As we can see, $\alpha = 2\delta e/3\sigma_r^2$ does not exceed 2% for $r \geq 0.1a$, i.e., the average kinetic energy of the particles exceeds the binding energy by more than 50 times.

Thus, the clump grows (or even stability) is out of the question: the clump flies apart in a time $\sim r/\sigma(l) \ll \tau_d(l)$, and its particles are randomly spread over the halo at radius $\sim l$ in a time $\sim \tau_d(l)$. However, their traces remain in the phase space of the system (Binney & Tremaine 2008): some particles are accelerated and some particles are decelerated by the gravitational field of initial Poisson noise, and so their integrals of motion are perturbed with respect to the exact analytical solution. Equation 11 allows us to estimate the integral variations via this effect. Indeed, $\alpha \approx \delta e/\sigma_r^2 = \delta(v^2/2)/\sigma_r^2 \approx v\delta v/\sigma_r^2 \approx \delta v/v$. It means that the ratio error of the particle speed occurring as a result of the Poisson noise is $\sim 2\%$ at $r \sim 0.1a$ and decreases with radius. The same estimation is valid for the ratio errors of the integrals of motion.

Thus, the simulations of a formes halo are not that sensitive to the Poisson noise, as a result of significant velocity dispersion in the formed halo, and stochastically generated initial conditions may be quite acceptable in this case. Below we will revert to the influence of the Poisson noise in our simulations.

3. Data treatment

First of all, we considered the velocity distribution of the particles at various radii and temporal moments and found no anisotropy: the initial isotropy of the velocity distribution conserves. We ignore all the data inside $0.1a = 10$ pc, i.e., $\sim 6\epsilon$ (or $\sim 3\epsilon$ for the second simulation with 10^5 particles) from the halo center in order to avoid the influence of the potential softening on the cusp. Moreover, our statistics is poor in this region.

In order to consider the density profile evolution, we split the halo into spherically symmetric layers of the same thickness

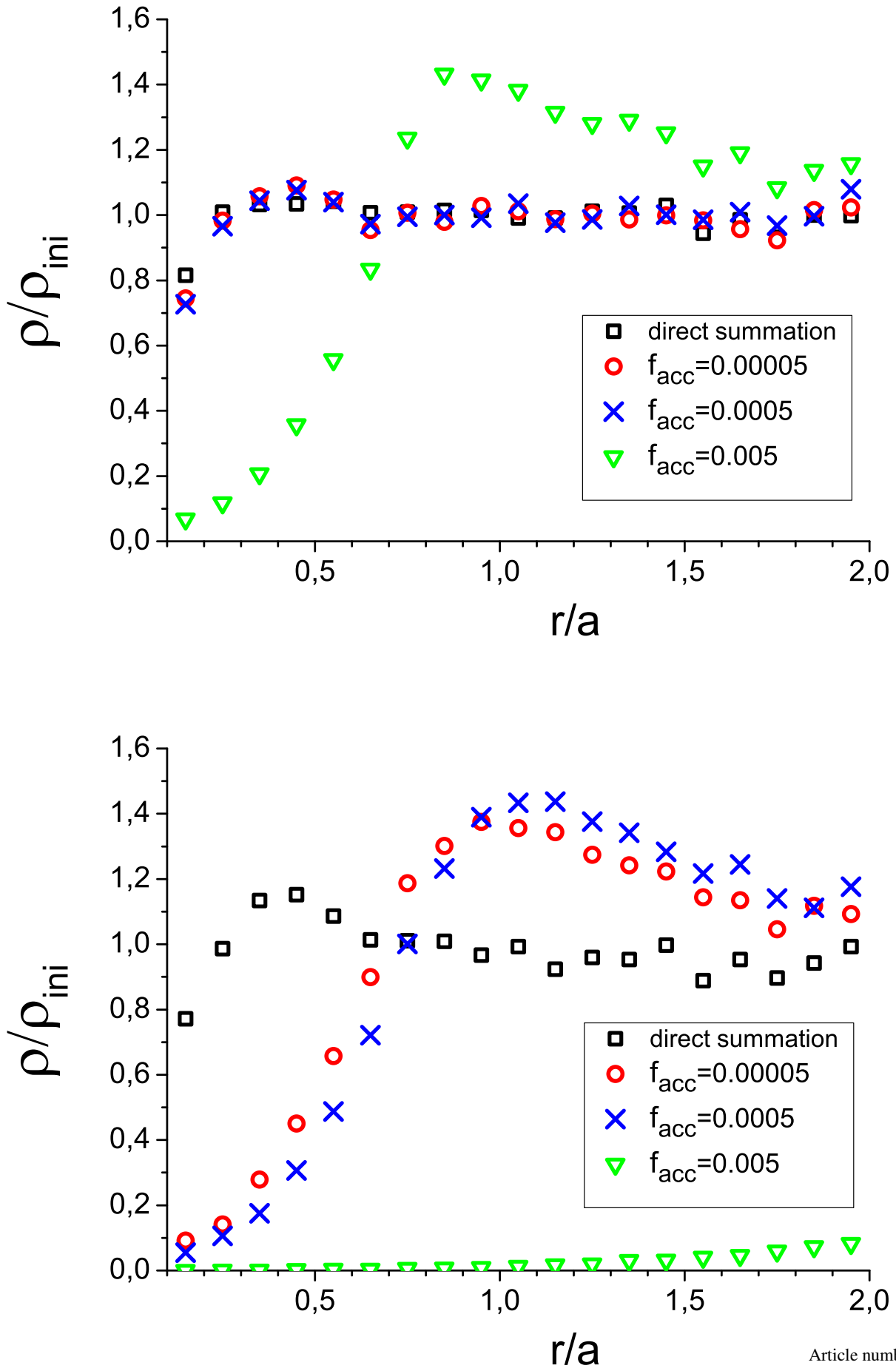


Fig. 2. The density profiles at $t = 0.45 \cdot 10^9$ years = 0.45 Gyr (top panel) and $t = 2.85 \cdot 10^9$ years = 2.85 Gyr (bottom panel). Black squares, red circles, blue crosses, and green triangles correspond to the direct summation (ph4 code), $f_{acc} = 5 \cdot 10^{-5}$, $5 \cdot 10^{-4}$, and $5 \cdot 10^{-3}$, respectively.

10pc = 0.1a and divide the number of particles in each by the value corresponding to the initial Hernquist profile (3). Thus we obtain an approximation of the current halo density as a fraction of the initial density $\rho_{ini}(r)$ given by the equation (3).

We want to consider variations of the integrals of motion and their dependence of radius. We split the 10^5 particles in simulations into groups of 1600 units in each, according to their initial r_0 , starting from the lowest r_0 . Thus, all the particles in the same group have similar r_0 . In principle, the group may be characterized by the averaged initial \bar{r}_0 of its members. Indeed, if the particle orbit is elongated, the particle spends almost all the time near the apocenter, in accordance with the Kepler's second law. On the contrary, if the orbit is circular, the particle moves along almost uniformly, but its radius always remains close to r_0 . However, each particle contributes to the density profile on an interval between its pericenter radius r_{min} and apocenter radius r_0 . Therefore, we use the averaged initial radius of the particles of the group \bar{r}_{ini} as the characteristic radius corresponding to the group. This choice is not very important: $\bar{r}_{ini} \lesssim \bar{r}_0$ for each group.

We examine the behavior of five integrals of motion: K , K_x , K_y , K_z , and r_0 . Let us use K to illustrate the procedure. At various given temporal moments, we calculate the change ΔK of K with respect to the initial value for each particle of a group. Then we evaluate the mean $\mu(\Delta K)$ and the standard deviation $\sigma(\Delta K)$ over the group.

To visualize the significance of the variations of the integrals of motion, we transfer to dimensionless values. We divide the mean changes μ and σ , relating to the angular momenta and their components, by $K_{circ}(\bar{r}_0)$, the angular momentum corresponding to the circular orbit at \bar{r}_0 . Roughly speaking, $K_{circ}(\bar{r}_0)$ is the maximum value of K any particle with the apocenter distance \bar{r}_0 may possess. We divide the mean changes $\mu(\Delta r_0)$ and $\sigma(\Delta r_0)$ by \bar{r}_0 . Being so defined, the values of μ and σ give us the idea of the importance of the non-conservation of the integrals of motion at various moments of time.

The non-conservation of integrals of motion leads to the Fokker-Planck diffusion of particles in the phase space. Indeed, (Baushev et al. 2017) found strong Fokker-Planck streams in the cusp area, which suggested that the numerical effect of alteration of the integrals of motion might significantly influence the shape of the cusp or even create it.

In order to investigate the point, we follow the procedure offered in (Baushev et al. 2017). For an array of radii r , we calculate the number $N_+(t, r)$ of particles that have $r_0 < r$ at the initial moment and $r_0 > r$ at the time t , and the number $N_-(t, r)$ of particles that have $r_0 > r$ at the initial moment and $r_0 < r$ at the time t . By counting each particle no more than once, we avoid a possible effect of small noise, produced by particles having r_0 just near the boundary radius r , crossing and recrossing it and thus giving an impression of intensive flows that do not exist. On the other hand, the values of $N_+(t, r)$ and $N_-(t, r)$ give only the lower bounds on the upward and downward Fokker-Planck streams of particles: the value of r_0 of a particle could have crossed r an odd number of times (and then it is counted only once) or an even number of times (and then it is not counted at all). In the collision-less case, $N_+(t, r)$ and $N_-(t, r)$ are obligatory equal to zero, since r_0 is an integral of motion.

4. Results and Discussion

Before discussing the obtained results, it is pertinent to remind briefly the main possible sources of numerical effects and the differences between the N-body codes we use. The discretization may lead to numerical artefact occurrence, the collisional

relaxation being one of them. All the simulations we perform in this work are equivalent in this sense, since the initial conditions (in particular, the number of particles in the halo) are exactly the same, and the potential softening is identical (which means that the Coulomb logarithm $\ln \Lambda$ has the same value). N-body codes typically use relatively simple algorithms of particle trajectory evaluation, for calculation duration's sake, which may also lead to numerical effects. However, GADGET-2 and ph4 use the same leapfrog algorithm. Thus, the only significant difference between the four simulations of the same halo that we perform in this work is the potential calculation algorithm. The most precise is the direct summation algorithm realized in ph4. The accuracy of the tree algorithm of GADGET-2 code depends on the cell-opening parameter f_{acc} : augmentation of f_{acc} makes the algorithm faster, but increases the numerical effects as well. We use three values: $f_{acc} = 5 \cdot 10^{-5}$, $5 \cdot 10^{-4}$, and $5 \cdot 10^{-3}$; the last one is typical for cosmological N-body simulations.

4.1. Density profiles and convergence criteria of N-body simulations

Figure (2) represents the density profiles (obtained with the help of the procedure described in the previous section) at $t = 0.45 \cdot 10^9$ years = 0.45 Gyr and 2.85 Gyr. Black squares, red circles, blue crosses, and green triangles correspond to the direct summation (ph4 code), $f_{acc} = 5 \cdot 10^{-5}$, $5 \cdot 10^{-4}$, and $5 \cdot 10^{-3}$, respectively.

We can see that the cusp behavior drastically depend on the potential calculation algorithm. The top panel in figure (2) corresponds to $\sim \tau_r$ at the radius $0.6a$ and to the Power's time $\tau_p = 1.7\tau_r$ at the radius $0.45a$ (the relaxation and Power's times scale with radius in accordance with (6)). The profiles calculated by the ph4 code and by GADGET-2 with $f_{acc} = 5 \cdot 10^{-5}$ and $f_{acc} = 5 \cdot 10^{-4}$ are still very similar and show yet no core, just a small drawdown in the center. A clear core with radius $r_{core} \simeq 0.6a$ forms in the case of the GADGET-2 code with $f_{acc} = 5 \cdot 10^{-3}$.

The bottom panel in figure (2) corresponds to $\sim \tau_r$ at the radius $1.45a$ and to the Power's time τ_p at the radius $1.1a$. The core radius is $r_{core} \simeq 0.6a$ for $f_{acc} = 5 \cdot 10^{-5}$ and $f_{acc} = 5 \cdot 10^{-4}$, and exceeds $2a$ for $f_{acc} = 5 \cdot 10^{-3}$. We should make a remark that, though the central part of the density profile corresponding to $5 \cdot 10^{-3}$ seems to be completely emptied at the bottom panel of figure (2), the absolute value of density still has a high peak in the center in this case. The impression of emptiness occurs because the density drops very significantly with respect to the initial cuspy profile. The most impressing fact is that the core does not form at all if we use the ph4 code: $\sim 14\tau_r$ have already passed at $r = 0.4a$, and there is no sign of core there. We can see only a small central drawdown.

We may make several conclusions from the plots. First, while the GADGET-2 profiles corresponding to $f_{acc} = 5 \cdot 10^{-5}$ and $f_{acc} = 5 \cdot 10^{-4}$ and the ph4 profile branch off after ~ 1 Gyr, the behavior of the profiles for the GADGET-2 simulations with $f_{acc} = 5 \cdot 10^{-5}$ and $f_{acc} = 5 \cdot 10^{-4}$ is identical. On the one hand, this might be a hint that a decreasing of f_{acc} below $5 \cdot 10^{-4}$ is not effective: it significantly increases the evaluation time and does not improve the result (at least, for the system under consideration). On the other hand, there is a popular way to check the simulation convergence: vary the simulation parameters by several times and (provided that the simulation results do not change) consider it as a prove of the simulation reliability. A comparison with the results of the direct summation algorithm shows that

the criterion fails in our case: though the decreasing of f_{acc} from $5 \cdot 10^{-4}$ to $5 \cdot 10^{-5}$ does not change the simulation results, the direct summation algorithm is still much better.

Second, the core formation occurs a bit earlier, but almost exactly as reported in (Power et al. 2003) if $f_{\text{acc}} = 5 \cdot 10^{-3}$. The core forms much later than the Power's time if $f_{\text{acc}} = 5 \cdot 10^{-4}$ or $5 \cdot 10^{-5}$. This is not surprising: $f_{\text{acc}} = 10^{-3}$ was used by (Power et al. 2003).

The third and the main conclusion is that (contrary to contrary to popular belief) the core formation in the halo centers in cosmological N-body simulations has nothing to do with the collisional relaxation of particles, being totally defined by the characteristics of the evaluation algorithm of gravitational field. Indeed, the collisional relaxation should manifest itself in exactly the same way for all the values of f_{acc} : we have exactly the same number and masses of particles, and exactly the same initial distribution. The softening radius ϵ is also the same, and so is the Coulomb logarithm $\ln \Lambda$. Nevertheless, the profile behaviors are completely different, i.e., they are defined by the value of the tree algorithm parameter f_{acc} , and not by the collisional relaxation.

This illustrates the failure of the generally recognized criteria (Power et al. 2003) of N-body simulation reliability, based on the profile stability and universality. Indeed, the cusp is routinely formed in the halo centers, being quite insensitive to the numerical code realization and initial conditions, then it remains stable until $t \sim 1.7\tau_r(r)$, and then a core appears. It is widely believed that the cusp stability and universality proves the negligibility of numerical effects until $t \sim 1.7\tau_r(r)$, while the core formation is the first manifestation of numerical effects (namely, of the collisional relaxation).

However, as we could see, the start of the core formation has nothing to do with the collisional relaxation; it is mainly defined by the properties of the tree algorithm, and can be strongly postponed or even avoided by the use of the direct summation algorithm `ph4`. As for the numerical effects, we will see in the next subsection that they become quite tangible on the time scale $\sim \tau_d(r)$, i.e., orders of magnitude earlier than the core formation. Thus, the commonly-accepted use of the central core formation as the first sign of presence of numerical effects breaks down. As we will see, the cusp formation itself is probably due to numerical effects.

4.2. Numerical 'violent relaxation'

The second interesting effect appearing in the simulations is an early occurrence of an instability. Figure (3) represents the density profiles of the system at $t = 32.1 \cdot 10^3 \text{ years} = 32.1 \text{ kyr}$, 564 kyr , $1.0 \cdot 10^6 \text{ years} = 1.0 \text{ Myr}$, and 5.64 Myr . Distinct 'waves' in the density profiles occur already at 32.1 kyr and reach the maximum amplitude at $\sim 1.0 \text{ Myr}$. After that, the amplitude of the instability does not change much: the perturbations do not grow and do not disappear. The 'waves' are in evidence in figure (2) as well. It is remarkable that the instability does not differ for all four values of f_{acc} that we used: the positions and the amplitudes of the 'waves' are identical. The amplitude also does not depend on the softening parameter.

We may also make another important conclusion from figure (3): the instability has nothing to do with the Poisson noise, or, more generally, any transient effects before the initial conditions settle into an equilibrium configuration. First, the waves are just too strong, their amplitude is $\sim 10\%$, while we may expect from equation 11 the amplitude $< 2\%$. Second, the Hernquist profile is stable, and tidal effects and dynamical friction tend to destroy any small substructures like the density waves

(Binney & Tremaine 2008). As we could see in section 2.3, the overdensities with small density contrast are easily destroyed by tidal effects. Nevertheless, the waves survive and even grow. Third, we performed the auxiliary simulation with the same number of particles, but with the doubled softening length and independently generated initial conditions (right panel in figure (3)). The positions of the Poisson clumps are quite different in this case, but the waves look quite similar, and even the positions of some of them are the same as in the main simulation. It suggests that the instability does not depend either from the softening radius, nor from the Poisson noise in the initial conditions.

We consider the behavior of the mean (μ) and mean-square-root (σ) variations of the integrals of motion, as we described in the previous section. It turns out that for all the integrals at all radii the mean variation is, at least, one or (more typically) two orders of magnitude smaller than the mean-square-root variation⁴. It means that the simulation codes conserve the net angular momenta and energy much better, than the characteristics of individual particles.

The temporal behavior of variations of K , K_x , K_y , K_z turns out to be almost indistinguishable (and, of course, $\sigma(\Delta K_x) \simeq \sigma(\Delta K_y) \simeq \sigma(\Delta K_z) \simeq \sigma(\Delta K)/\sqrt{3}$). Therefore, we present the results only for K instead of that for K_x , K_y , K_z . What is more, the temporal behavior of all the five integrals is also very similar for the `GADGET-2` and `ph4` simulations, especially the results for the tree simulations with the `GADGET-2`, which are almost identical. Therefore, we plot only the results for the direct summation (black crosses) and `GADGET-2` with $f_{\text{acc}} = 5 \cdot 10^{-3}$, since they differ the most.

Figure (4) represents the behavior of $\sigma(\Delta K)$ (left panel) and $\sigma(\Delta r_0)$ (right panel) at the radii $r = a/2$ (upper panel) and $r = 2a$ (lower panel). As we can see, even the behaviors of $\sigma(\Delta K)$ and $\sigma(\Delta r_0)$ are quite similar: they linearly grow with time, then reach their maximum at $t \sim \tau_d(r)$, then slightly decrease, and then grow again, but significantly slower. The temporal behavior resembles that of the above-discussed instability of the density profile (figure (3)), and it is more than proper to assume that this is actually the same phenomenon.

Finally, the instability is quite distinct in figures (5) and (6) representing the upward $N_+(t)$ (black crosses) and downward $N_-(t)$ (red circles) radial streams of particles through the spheres⁵ of radii $r = a/2$ and $r = 2a$, respectively, divided by the total number of the particles $N(r)$ inside r . The separation of the cross and circle lines at the late parts of the plots corresponds to the core formation and has nothing to do with the instability. However, other features of the plot closely resemble these of the figure (4): $N_+(t)$ and $N_-(t)$ (the number of particles, which apocenter distances r_0 have crossed the spheres of radii $r = a/2$ and $r = 2a$) rapidly grow with time, then reach their maximum at $t \sim \tau_d(r)$, then slightly decrease, then some particles even return back ($N_+(t)$ and $N_-(t)$ decrease), and then grow again, but significantly slower.

⁴ Except of the trivial case, when the core forms, and a lot of particles collectively leave the center. However, the core formation occurs relatively late, and we can easily avoid the influence of this effect, just disregarding the data after its beginning.

⁵ See section 3 for exact definitions of the streams.

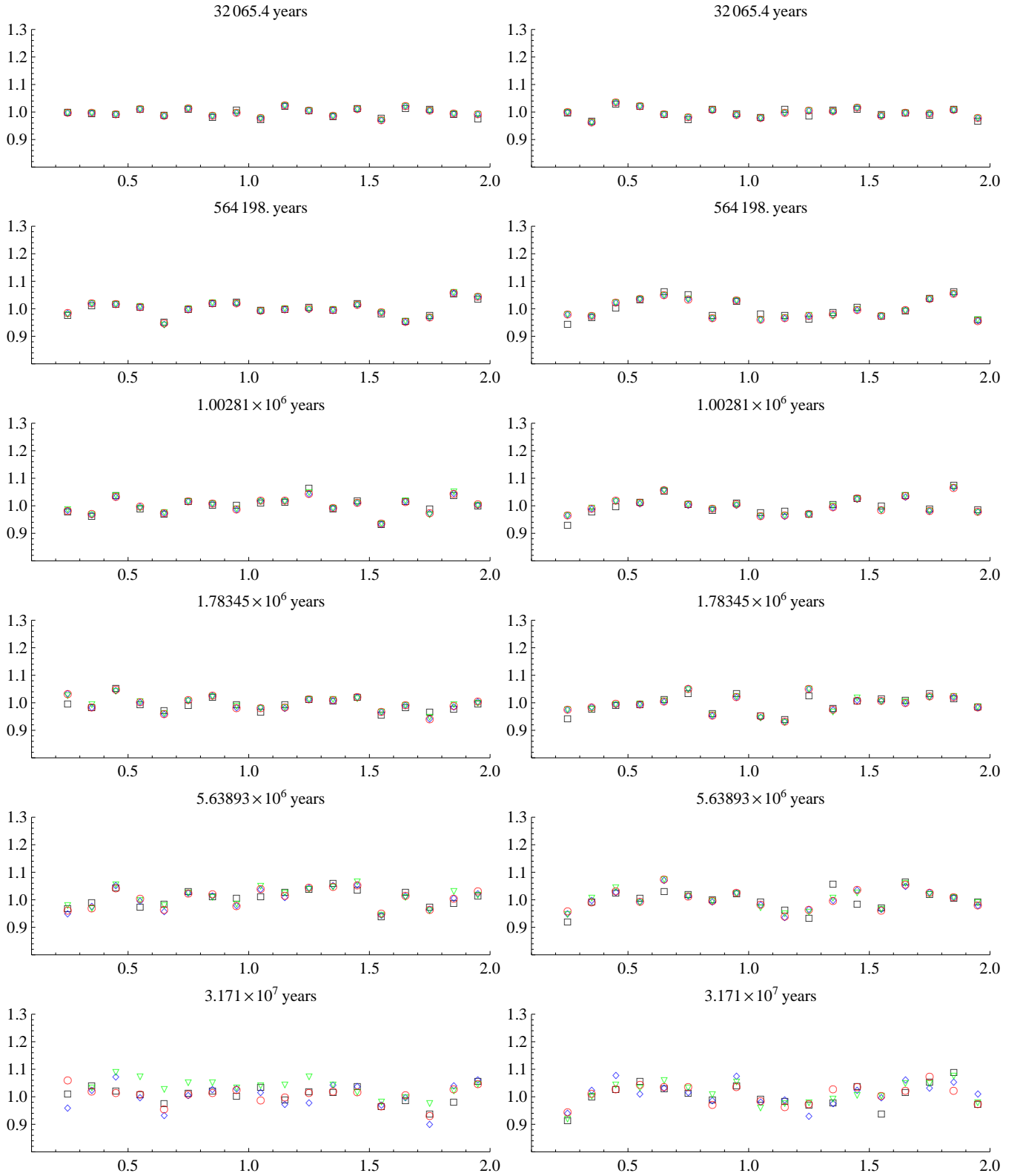


Fig. 3. The density profiles at $t = 32.1 \cdot 10^3$ years = 0.321 kyr, 564 kyr, $1.0 \cdot 10^6$ years = 1 Myr, 1.78 Myr, 5.64 Myr, and 31.7 Myr (see the top caption of each plot) for the main simulation with 10^5 particles (left plots), and the auxiliary simulation with the same number of particles (10^5), doubled softening length $\epsilon = 3.4$ pc, and the independently generated initial conditions (right plots). Black squares, red circles, blue diamonds, and green triangles correspond to the direct summation (ph4 code), $f_{acc} = 5 \cdot 10^{-5}$, $5 \cdot 10^{-4}$, and $5 \cdot 10^{-3}$, respectively.

The behavior of the quantities presented in figures (4), (5), and (6) clearly indicates that the rapid initial variations of the integrals of motion are not due to a slow accumulation of numerical inaccuracies or the collisional relaxation: first, the decrease of the standard deviations (figure 4), as well as the decrease of the number of particles having crossed the radii $r = a/2$ (figure 5) and $r = 2a$ (figure 6), at $t \sim \tau_d(r)$ would be impossible in this case. Second, the standard deviations in figure (4) grows linearly for $t < \tau_d(r)$, which suggests that we deal with a collective instability, and not with any sort of a stochastic process. Indeed, in figure 3 we can see the appearance of density waves with the amplitude corresponding to that of the integrals variations.

We should emphasize that *the instability is undeniably a numerical effect*. The Doremus-Feix-Baumann theorem together with the Antonov's second law (see (Binney & Tremaine 2008) for details) prove: the Hernquist profile with the isotropic velocity distribution that we model is stable.

What could be the influence of the instability on the cosmological simulations, in particular, the simulations of the hierarchical structure formation? We will discuss this question in more details in the next subsection, here restricting ourselves to a remark that the effect that we have found resembles the violent relaxation (Lynden-Bell 1967) (hereafter we abbreviate it as VR), which may occur during the halo formation from an initial small perturbation. The essence of later process is simple: when the halo collapses, strong and rapidly evolving density inhomogeneities (caustics etc.) should appear. The inhomogeneities create a small-scale gravitational field, and as a result the halo particles may effectively exchange their energies and other integrals of motion. The characteristic time of the violent relaxation $t \sim \tau_d(r)$ coincides with that of the instability that we have found: the violent relaxation 'works' only during the halo collapse.

However, the real violent relaxation has nothing to do with the numerical 'violent relaxation' that we have found. The violent relaxation is a quite real effect that may occur (but not necessarily occurs) during the halo formation. It certainly cannot take place in our simulations, since we consider a stationary and stable profile. There are also less fundamental differences between the effects: for instance, the efficiency of the violent relaxation rapidly drops with radius, while figure (3) shows that the numerical 'violent relaxation' is rather effective even at large radii.

A major challenge for N-body simulations is that there seems to be no apparent way to separate the real and numerical violent relaxations in realistic cosmological modelling. Furthermore, as we will see, the numerical relaxation in simulations of the hierarchical structure formations may, in all likelihood, be far in excess of the $\sim 10\%$ that we obtain for the stationary halo and completely transfigure the energy portrait of the system.

We may say a few words about the nature of the instability. Since its development is not sensitive to f_{acc} , the instability does not depend on the algorithm of gravitational field evaluation. It is hardly an effect of discretization: if this were so, the effect would drastically depend of radius (as, for instance, the collisional relaxation does). The phenomenon is probably produced either by an inadequate accuracy of the trajectory evaluation algorithm, or by the Miller's instability.

Actually, it is the Miller's instability (together with the calculation time) that makes an employment of precise and heavy algorithms of trajectory evaluation in N-body simulations low useful: the Miller's instability makes the Liapunov time comparable with the dynamical time of the system (Miller 1964). Even if we take into account the specificity of N-body algorithms (like the potential smoothing), the instability arises in a time, which

is much shorter than $\tau_r(r)$ at the given radius and remains comparable with the dynamical time $\tau_d(r)$ (Valluri & Merritt 2000; Hut & Heggie 2002). The credence to the results of N-body simulations under these conditions is totally based on the resulting density profile stability. Indeed, different N-body codes, with various algorithms of potential and trajectory evaluation lead to quite similar profiles of the formed halos. Relying on this, the profile is considered to be physically meaningful and describing real halos, despite of the fact that the orbits of individual particles have no physical significance (Binney & Tremaine 2008, section 4.7.1(b)). Now we try to show on the basis of our simulations, how vulnerable this reasoning is.

4.3. The variations of the integrals of motion and the 'core-cusp problem'

4.3.1. Are the variations of integrals of motion of individual particles important?

Thus we have found that, on the one hand, the integrals of motion of individual particles significantly vary in a short time (they change on $\sim 10\%$ in $\sim 10^6$ years, i.e., $\sim 10^{-4}$ of the age of the Universe). On the other hand, the density profile is, generally speaking, quite stable and does not decline much from the analytical solution. This raises a very important question. It is widely believed that, though the Miller's instability totally ruins the orbits and the integrals of motion of individual particles, the statistical properties of the particle distribution (in particular, the density profiles) are trustable. Indeed, N-body simulations of the clustering of dark matter lead to a universal density profile of the halos (hereafter we abbreviate it as UDP), low-sensitive to the simulation parameters (Power et al. 2003). Unfortunately there is no adequate analytical model of the clustering, and we cannot compare the simulation results with the analytical solution. However, the fact that different computer codes lead to very similar UDPs (though the UDP itself gradually changes from the NFW in 1997 to the Einasto profile with $n \simeq 6$ in 2017) creates an impression that the DM density profiles may be reliably simulated despite of inaccuracies of the velocity distribution and any dynamical parameters of individual particles (Gao et al. 2008; Dutton & Macciò 2014).

Of course, this is not true. First, the velocity distribution is mutually bound with the density profile. For simplicity, let us consider a stationary spherically symmetric DM halo with an anisotropic velocity distribution of the particles. Then the particle distribution f in the phase space is a function of only the particle energy w (Binney & Tremaine 2008): $f(r, \mathbf{v}) \equiv f(w) = f(\phi(r) + v^2/2)$. The velocity distribution and the density at some radius r are equal to $f(\phi(r) + v^2/2)dv^3$ and $\int 4\pi v^2 f(\phi(r) + v^2/2)dv$, respectively. Thus, any inaccuracy of the velocity distribution directly translates into an inaccuracy of the density profile.

The second, more fundamental argument is the following. We consider a spherically symmetric halo; therefore, we may use the integrals of motion K , K_x , K_y , K_z , and r_0 as a full set of generalized coordinates⁶ and consider the distribution function f of the system as a function of only these five coordinates. A collisionless system (for instance, a DM system, which is supposed to be collisionless) obeys the collisionless kinetic equation $df/dt = 0$. On the other hand, if the integrals of motion experience a relatively slow evolution (which is the case), the system may be described by the Fokker-Planck equation

⁶ Actually, we may even get rid of one of the integrals K , K_x , K_y , K_z , since they are bound by the trivial equation $K^2 = K_x^2 + K_y^2 + K_z^2$.

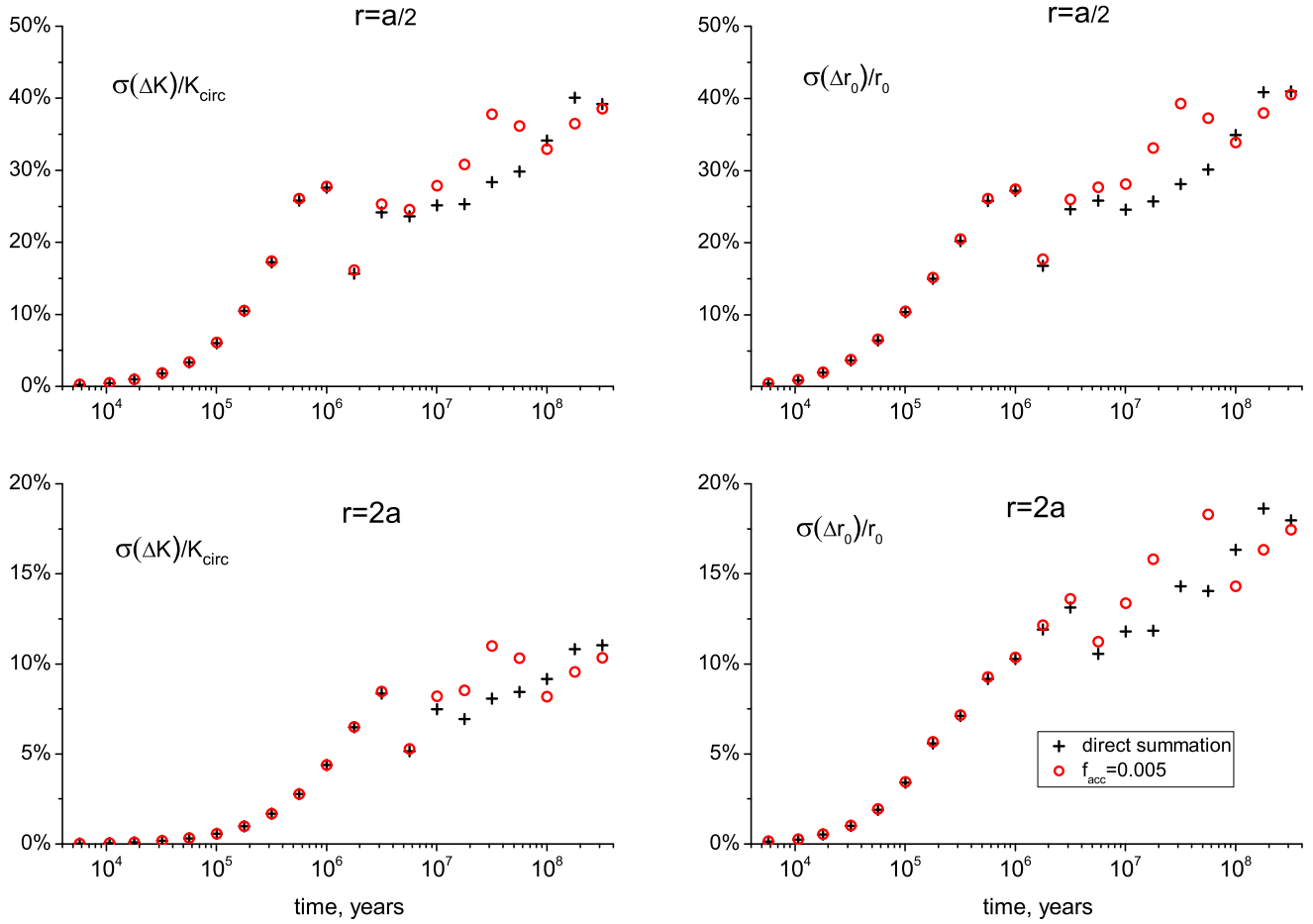


Fig. 4. The temporal behavior of $\sigma(\Delta K)/K_{\text{circ}}$ (left panel) and $\sigma(\Delta r_0)/\overline{r_0}$ (right panel) at the radii $r = a/2$ (upper panel) and $r = 2a$ (lower panel) for the direct summation algorithm (ph4, black crosses) and GADGET-2 with $f_{\text{acc}} = 5 \cdot 10^{-3}$ (red circles).

(Landau & Lifshitz 1980)

$$\frac{df}{dt} = \frac{\partial}{\partial q_\alpha} \left\{ A_\alpha f + \frac{\partial}{\partial q_\beta} [B_{\alpha\beta} f] \right\} \quad (12)$$

where q_α are the integrals of motion, and A and B are the Fokker-Planck coefficients.

$$A_\alpha = \overline{\frac{\delta q_\alpha}{\delta t}} \quad B_{\alpha\beta} = \overline{\frac{\delta q_\alpha \delta q_\beta}{2\delta t}}. \quad (13)$$

Figure (4) illustrates that at least some of B s tangibly differ from zero. Hence the N-body system in all our simulations behave as essentially collisional.

Thus, a reliable simulation of DM density profiles without a reliable simulation of the velocity distribution and the integrals of motion of individual particles is out of the question.

4.3.2. The 'core-cusp problem' and the halo relaxation

The 'core-cusp problem' gives us an apt illustration of the importance of correct modelling of the behavior of the integrals of motion (in particular, of the particle energies) in simulations for reliability of their results. Indeed, DM halos appear from small linear cosmological perturbations. It is easy to show analytically that a strong relaxation is absolutely necessary during the halo formation in order to form a cuspy profile; the resulting profile is

obligatory cored if the relaxation is moderate or weak (Baushev 2014a,b). Fundamentally, the only plausible mechanism of the strong relaxation during the formation of a DM halo is the violent relaxation⁷. However, it is important to understand, how effective the real VR is, i.e., how significantly the initial specific energy is redistributed between the DM particles during the formation of an astrophysical halo. The task of the gravitational collapse is too complex to obtain an exact analytical solution for realistic situations. Observations rather suggest that the relaxation is not violent (Baushev 2014b). And our simulations show that a numerical 'violent relaxation' occurs in the N-body modelling, which may be easily confused with the real VR.

There is no apparent way to control the integrals of motion in real cosmological simulations, but we model the Hernquist profile, which is very close the universal density profile obtained in cosmological simulations. We find the change of the integrals on $\sim 10\%$ in the time interval of $\sim 10^{-4}$ of the age of the Universe. Though the integrals of motion evolve much slower after the initial 'violent relaxation', we should emphasize that

⁷ In principle, barionic matter may also participate in the relaxation of real astrophysical halos. However, we discuss the 'core-cusp problem', which is the most acute just in the case of halos that contain an unusually small fraction of barionic matter, like dwarf spheroidals (Walker & Peñarrubia 2011). Therefore, it is unlikely that taking account of the barionic matter influence may resolve the 'core-cusp problem' (Oman et al. 2015).

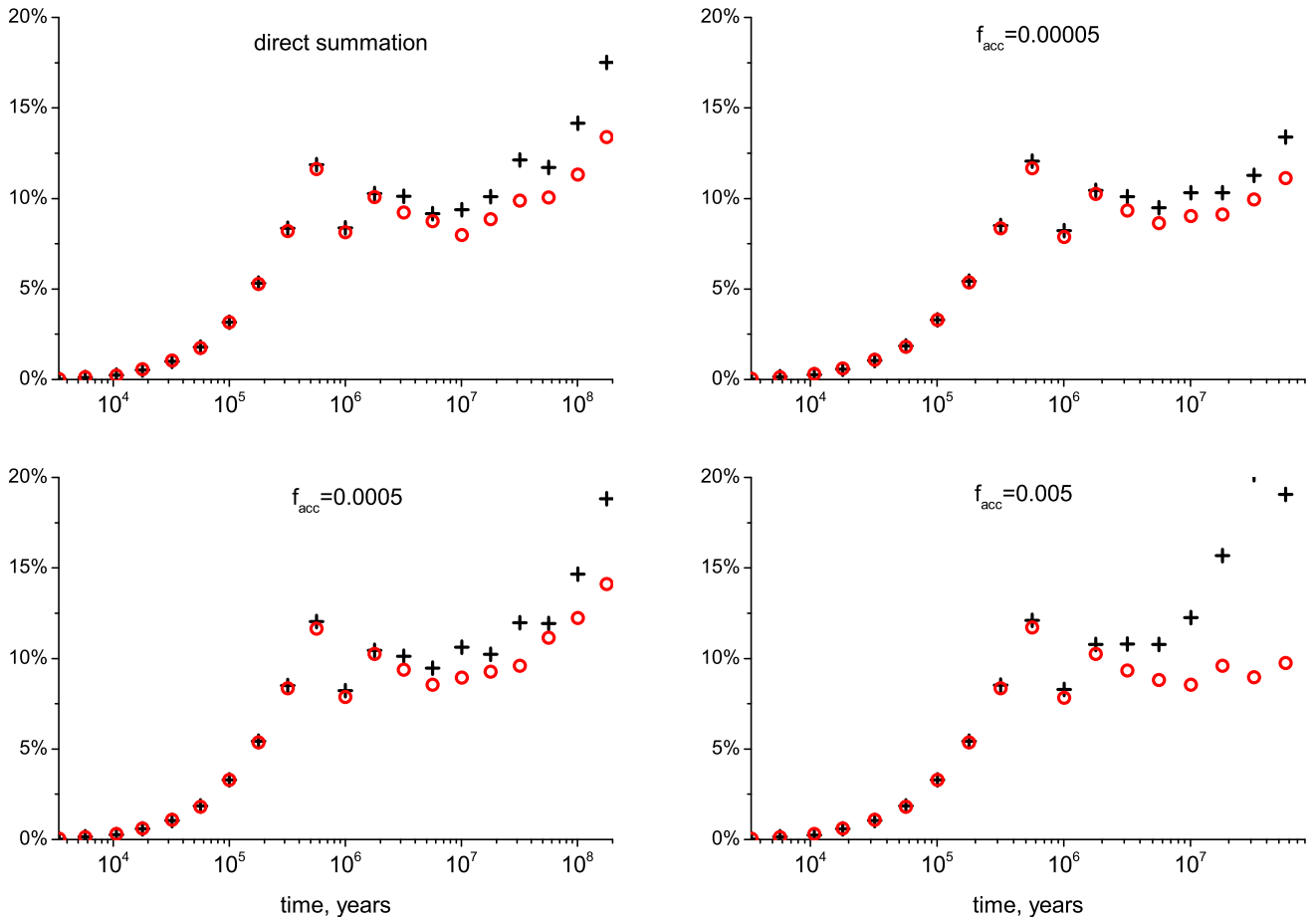


Fig. 5. The upward $N_+(t)$ (black crosses) and downward $N_-(t)$ (red circles) radial streams of particles (see section 3 for exact definition) through the sphere of radius $r = a/2$, divided by the total number of the particles $N(a/2)$ inside $a/2$.

the numerical artefacts in simulations of the hierarchical structure formations may, in all likelihood, be far in excess. First, we model an ideal system, a stationary halo. Second, the effects of the 'numerical interaction' between particles occurring in complex simulations of the hierarchical clustering are most likely to be more perceptible: the simulation inaccuracies may be larger during the highly-nonstationary process of halo collapse. Third, the numerical 'violent relaxation' may occur over and over again in repeating merging of smaller halos into a larger one during the hierarchical clustering. Fourth, the first halos always contain only few tens of particles, and later these first halos contribute to the cusps of more massive ones. We confront with a question: are the halos with small N simulated properly? This problem has been discussed in literature in the context of two-body relaxation (Binney & Knebe 2002), but if the numerical effects are already important at the dynamical time, the problem of the first halos may be much more important.

Hence the N-body simulations also give no plausible way to determine the efficiency of the relaxation occurring during the formation of astrophysical DM halos. A strong relaxation is absolutely necessary to form a cuspy profile from the initial small perturbation (Baushev 2014a,b), and it apparently occurs in N-body simulations. However, if the relaxation is real, the cusps routinely occurring in the centers of DM halos in cosmological N-body simulations correspond to the properties of real astrophysical systems. If the relaxation is caused by numerical effects

— the cusps are no more than a numerical artefact. In the first case, the 'core-cusp problem' gives us the extremely valuable information that cold DM paradigm is wrong: the DM should be either warm, or self-interacting, or has some other non-trivial physical properties. In the second case, we still need to improve N-body codes in order to be able to make physical conclusions from discrepancies of the simulation results and observations.

It is a wide-spread opinion (based mainly on (Power et al. 2003) and similar works) that the cusp formation in the centers of DM halos is a genuine property of collision-less systems: indeed, in N-body simulations it forms in a time, which is comparable with $\tau_d(r)$ and much shorter than $\tau_r(r)$. Meanwhile, the core formation at $t \approx 1.7\tau_r(r)$ is considered as the first sign of relaxation. Thus, it is believed that the relaxation tends to destroy the cusp.

Our simulations show that both these statements are doubtful. First, the core formation at $t \approx 1.7\tau_r$ is caused by inaccuracy of the tree algorithm, and not by a relaxation. Second, the density profiles corresponding to the direct summation code ph4 are almost identical in the upper and lower panels of figure (2), i.e., at time moments $t = 0.45$ Gyr and $t = 2.85$ Gyr. There is no core formation, and the profile for $r \geq 0.2a$ has little difference with the initial one. The small depression at $r \leq 0.1a$ is most likely not the core, but an effect of the potential softening: its radius is $\sim 6\epsilon$, and (contrary to the core) it does not grow with time. Meanwhile, the upper and lower panels of figure (2) correspond

to ~ 1.4 and $9\tau_r$ at $r = 0.5a$ and ~ 11 and $70\tau_r$ at $r = 0.2a$, respectively. The influence of, at least, the collisional relaxation should be very significant (or even decisive) at $t \sim 70\tau_r$. However, we can see no cusp destruction outside $r = 0.1a$ (contrary to the GADGET-2 simulations). Thus, the relaxation effects do not obligatorily tend to transform a cusp into a core. On the other hand, as we have already mentioned, a strong relaxation is necessary to form a cuspy profile from the initial small perturbation. Hence relaxation processes tend to form the cusp, rather than to destroy it.

4.3.3. The Fokker-Planck streams

The standpoint that the cusps in the halo centers is a numerical artefact is strongly supported by the properties of the upward $N_+(t, r)$ and downward $N_-(t, r)$ radial drifts of particles in the halo. As one can see in figure (5), $\sim 12\%$ of particles inside $r = a/2$ cross this radius in a quite short period of time $t \sim \tau_d$ (to be more precise, their apocenter distances r_0 cross $r = a/2$), and the halo profile is stable only because the upward and downward streams compensate each other. Indeed, the curves in figures (5) and (6) branch off at ~ 10 Myr, earlier in figure (5) and later in figure (6). The appearing imbalance between the upward and downward streams corresponds to the core formation. The divergence of the curves for the ph4 simulation (the upper left panels in both the figures) is rather small, which depicts the strong suppression of the core formation in this instance. It is interesting to mention that the N_+ and N_- curves branch off much earlier, than the moment when the core becomes visible in the density profile.

Let us underline several important points. First, the drifts N_+ and N_- are purely numerical effects: $N_+(t, r) = N_-(t, r) \equiv 0$ in the collisionless case, since r_0 is an integral of motion. Second, the streams are not just a minor effect of a low-amplitude particle wiggling: as we have already mentioned, each particle is counted no more than once in calculation of N_+ and N_- . What is more, the fluxes are just too strong. For instance, the number of particles crossing the radius $r = a/2$ in $t \approx \tau_d(a/2)$ (figure (5)) is approximately equal to the total number of particles between $a/2$ and $a/2 + 0.04a$. Thus, the orbits of particles move as a whole in the halo due to some significant numerical effects, and the amplitude of this drift is quite large on average.

It may be argued that, though the numerical streams under consideration are rather intensive, they are insufficient to determine the profile shape, since only $\sim 12\%$ of particles inside $r = a/2$ are carried through this sphere in $t \sim \tau_d(a/2)$, and then the streams significantly weaken. This is not so. First, the upper left panel in figure (5) (the only panel in the figure, where the influence of the core formation is relatively small) shows that N_+ and N_- are still growing after $t \sim \tau_d$, even if much slower than during the numerical 'violent relaxation'. They reach $\sim 15-20\%$ at $t = 0.2$ Gyr, and if their growth continues like this, they may reach $\sim 100\%$ at $t = 1.36$ Gyr. It means that the numerical effects may thoroughly redistribute the particles even inside the radius $r = a/2 = r_s$. Moreover, this radius is very large, the 'core-cusp problem' occurs much closer to the center, while the efficiency of the numerical streams grows in inverse proportion of radius.

We cannot reliably calculate $N_+(t, r)$ and $N_-(t, r)$ for $r \ll a/2$, because the core formation starts too early at small radii. Since we use the slow algorithm ph4, we have to limit ourselves with 10^5 particles in the halo. It spoils the spacial resolution, and the relaxation time becomes comparable with the dynamical one as we approach the halo center. However, we can estimate the behavior of $N_+(t, r)$ and $N_-(t, r)$ close to the halo

center if we combine our results with those of (Baushev et al. 2017). These authors also simulate the Hernquist halo, but they test only the Gadget-2 code with $f_{acc} = 0.005$. As a result, simulations (Baushev et al. 2017) contain much more particles and gain significantly higher spatial resolution. The authors of (Baushev et al. 2017) also found the unphysical streams $N_+(t, r)$ and $N_-(t, r)$, and in the area where we can compare the results, they coincide with ours. In the region between $r = 0.1a$ and $r = 0.5a$ the ratios $N_+(\tau_d, r)/N(r)$ and $N_-(\tau_d, r)/N(r)$ (i.e., the number of particles crossed the sphere of radius r upward and downward, respectively, in the dynamical time at this radius, divided by the total number of the particles $N(r)$ inside r) are in inverse proportion of r (see figure 3 in (Baushev et al. 2017)). It means that the fraction of particles carried by the unphysical streams through the sphere of radius $r = 0.1a = 0.2r_s$ in $t \sim \tau_d$ reaches $\sim 60\%$ of the total mass inside the sphere. Recall that we consider the ideal instance of a stationary and stable halo. If in the cosmological simulations of hierarchical structure formation the balance between the upward and downward streams is violated, the 60% mass drift is sufficient to transfigure the profile entirely, in particular, to form the cusp in $t \sim \tau_d$.

Hence a purely numerical effect, the upward and downward streams of particles, are strong enough to totally determine the shape of the density profile in the centers of cosmological halos. The profile is stable not due to the absence of numerical effects, but just due to the mutual compensation of two strong numerical artefacts. Moreover, we do not know for sure, why the upward N_+ and downward N_- streams initially compensate each other so well, and why the self-compensation ends at some moment leading to the core formation. One can see that the last process is defined by the parameters of N-body codes, having nothing to do with the properties of real DM systems. Besides this, the time of the numerical 'violent relaxation' that we found ($t \sim \tau_d$) coincides with the characteristic time ($\sim \tau_d$) of the central cusp formation in cosmological N-body simulations.

4.3.4. Resume

To summarize, the unphysical stream of particles N_- during the numerical 'violent relaxation' can bring through the radius $r = 0.1a = 0.2r_s$ approximately 60% of the mass that the resulting halo contains inside this radius. This is more than enough to form the cusp in the halo center in $t \sim \tau_d$ by purely numerical effects. The intensive variations of the integrals of motion of individual particles reveals a sort of interaction between them (it does not matter if it is physical or numerical), and the system is described not by the collision-less kinetic equation, but by the Fokker-Planck one. The Fokker-Planck equation has its own stationary solutions, and the universal density profile obtained in simulations falls exactly on the stationary solution of the Fokker-Planck equation in the halo center (Baushev & Barkov 2018; Baushev 2015). All these facts suggest that the cusp routinely occurring in the centers of DM halos in cosmological simulations is no more than a numerical artefact.

Finally, the 'core-cusp problem' is the most known, but not the only strange phenomenon occurring in N-body simulations. The authors of (van den Bosch et al. 2018; van den Bosch & Ogiya 2018) report that, in the absence of baryonic processes, the complete physical disruption of CDM substructure should be extremely rare⁸ and that most disruption in numerical simulations are, most likely, artificial. The authors suppose that subhaloes in N-body simulations suffer from an in-

⁸ Analytical consideration supports this statement (Baushev 2016).

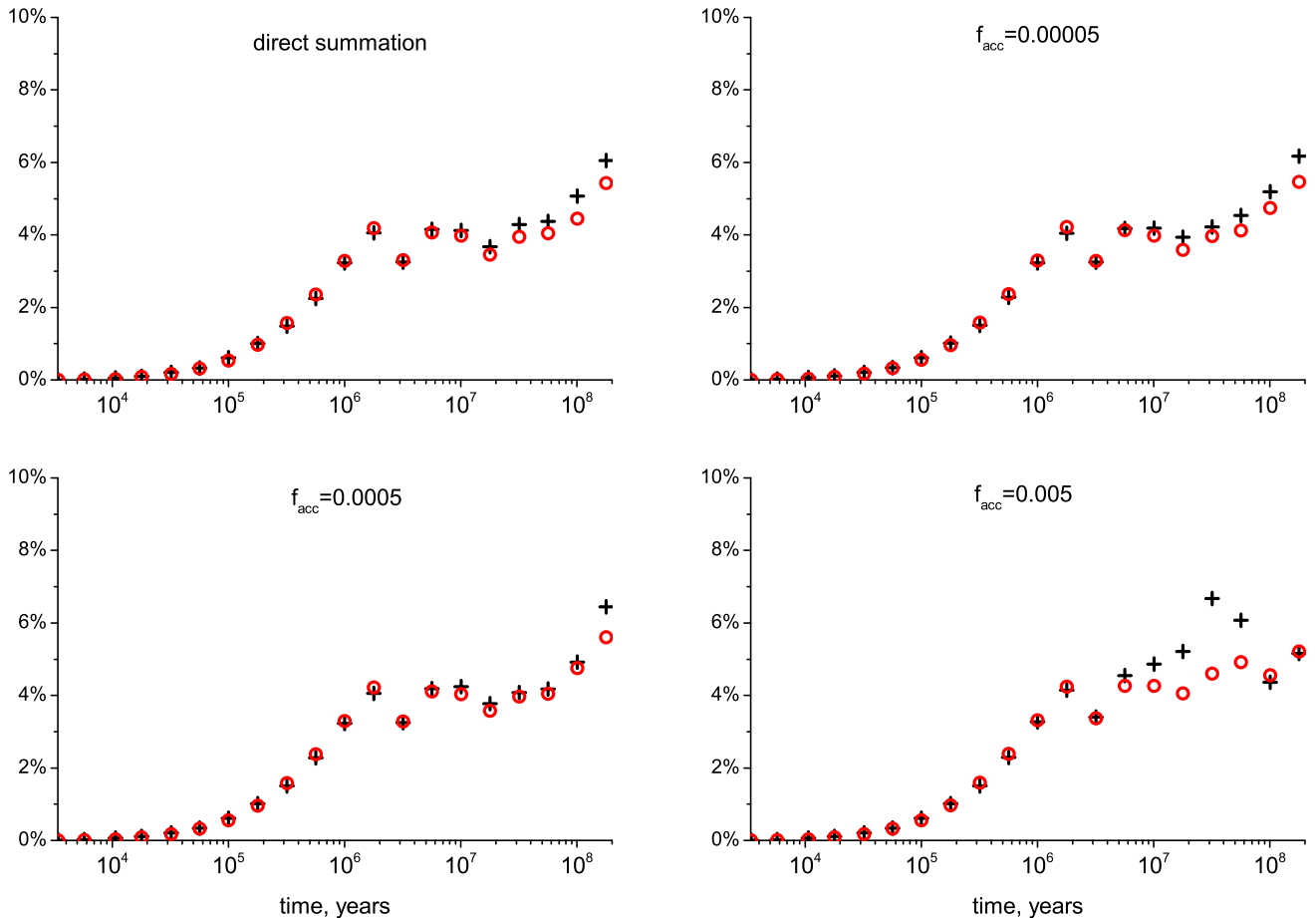


Fig. 6. The upward $N_+(t)$ (black crosses) and downward $N_-(t)$ (red circles) radial streams of particles (see section 3 for exact definition) through the sphere of radius $r = 2a$, divided by the total number of the particles $N(2a)$ inside $2a$.

stability triggered by the amplification of discreteness noise in the presence of a tidal field. We can see, however, that some numerical instability occurs even in a stationary and stable halo, and even in the absence of any tidal field.

The main conclusion that one can make from these facts is that the present state-of-art of N-body simulation tests is absolutely insufficient. First, the criteria of reliability based on the profile stability and universality are extremely questionable and may lead to false convergence, as we could see. The full set of integrals of motion of the system should be considered to reveal undesirable numerical effects with assurance. Yes, precise evaluation of trajectories of each particle is probably unnecessary to reliably reproduce the halo density profiles. However, the neglect of the energy and momentum exchange between particles is surely not harmless.

Second, one can see that the density profile in GADGET-2 simulations is unresponsive to decreasing of f_{acc} below $5 \cdot 10^{-4}$. Thus, we reach a sort of 'convergence', but the convergence is false: the behavior of the real DM system that we model (or even of the system where the gravitational force is evaluated with the help of the direct summation algorithm) is significantly different. This is a good illustration why a comparison of the simulation results with the analytical model should always be preferred over a comparison of the simulation results with another simulation results as a reliability test. Indeed, an analytical solution of the extremely complex task of the hierarchical structure formation is

scarcely possible. However, it is usually possible to offer an analytical model close enough to the realistic one. For instance, for each halo obtained in simulations, an analytical model of an isolated halo with similar profile and similar velocity distribution may always be obtained (Binney & Tremaine 2008), which allows to test the simulation properties comprehensively, with the use of the full set of dynamical parameters of the system. Only irreproachably reliable estimations of the simulation accuracy and convergence may permit to make strong physical conclusions: otherwise any discrepancy with observations may turn out to be just a result of an unaccounted numerical effect.

5. Summary

1. The reliability criteria of the N-body simulations based on the profile stability and universality (like (Power et al. 2003)) are unsafe. In particular, the opinion that the universal density profile (UDP) commonly occurring in the cosmological simulations corresponds to the absence of any significant numerical effects, while the core formation in the center is a result and the first sign of the collisional relaxation, is absolutely incorrect. First, very essential numerical effects occur much earlier than the core formation. Second, the core formation has nothing to do with the collisional relaxation, being defined by the parameters of the tree algorithm. Thus, the criteria like $t \leq 1.7\tau_r(r)$ are based on artificial binding of

- two essentially independent processes and therefore cannot be valid.
2. An instability with the characteristic time $\sim \tau_d(r)$ develops immediately after the simulation launch. It leads to a numerical 'violent relaxation': the integrals of motion change (on the average) on 10% from their initial values even at $r \approx r_s$. In contrast to the real violent relaxation (Lynden-Bell 1967), the relaxation that we found is purely numerical. The mechanism of its occurrence is not quite clear; most likely, this is a result of either an inadequate accuracy of the trajectory evaluation algorithm, or the Miller's instability.
 3. Relying on the present-day N-body simulations, one cannot infer that a relaxation (in particular, the collisional one) tends to transform a cusp into a core in the center of DM halos. Theoretical consideration rather suggests the opposite: a relaxation assists to the cusp formation, at least, during the halo formation.
 4. The necessity of a strong relaxation for a cuspy profile formation (Baushev 2014a,b) makes critical the issue of correct modelling of the initial halo relaxation in cosmological simulation. If the N-body simulations overestimate the relaxation during the halo formation (as a result of the numerical 'violent relaxation' that we found), it may lead to a false cusp formation in the halo center. Our results give every reason to believe that it is exactly what happens in the N-body simulations of the large-scale structure formation. Then the 'core-cusp problem' is no more than a technical problem of N-body simulations.
 5. The significant variations of the integrals of motion reveal that the system of test particles in the N-body simulations is essentially collisional, contrary to real DM systems. In the idealized case of a stationary and stable halo that we consider, the variations do not affect much the density profile, but their influence cannot be minor in simulations of the hierarchical structure formation of the Universe.
 6. Much remains to be done in testing of N-body simulation convergence and reliability. A comparison of the simulation results with the analytical model should always be preferred over a comparison of results of different simulations.

- Baushev, A. N., del Valle, L., Campusano, L. E., et al. 2017, *J. Cosmology Astropart. Phys.*, 5, 042
- Binney, J. & Knebe, A. 2002, *MNRAS*, 333, 378
- Binney, J. & Tremaine, S. 2008, *Galactic Dynamics: Second Edition* (Princeton University Press)
- Chemin, L., de Blok, W. J. G., & Mamon, G. A. 2011, *AJ*, 142, 109
- de Blok, W. J. G. 2010, *Advances in Astronomy*, 2010, 789293
- Dehnen, W. 2001, *MNRAS*, 324, 273
- Dutton, A. A. & Macciò, A. V. 2014, *MNRAS*, 441, 3359
- Evans, N. W. & Collett, J. L. 1997, *ApJ*, 480, L103
- Gao, L., Navarro, J. F., Cole, S., et al. 2008, *MNRAS*, 387, 536
- Harvey, D., Courbin, F., Kneib, J. P., & McCarthy, I. G. 2017, *MNRAS*, 472, 1972
- Hayashi, E., Navarro, J. F., Taylor, J. E., Stadel, J., & Quinn, T. 2003, *ApJ*, 584, 541
- Hénon, M. H. 1971, *Ap&SS*, 14, 151
- Hernquist, L. 1990, *ApJ*, 356, 359
- Hernquist, L. & Katz, N. 1989, *ApJS*, 70, 419
- Hut, P. & Heggie, D. C. 2002, *Journal of Statistical Physics*, 109, 1017
- Klypin, A., Prada, F., Yepes, G., Hess, S., & Gottlöber, S. 2013, *ArXiv e-prints*
- Knebe, A., Kravtsov, A. V., Gottlöber, S., & Klypin, A. A. 2000, *MNRAS*, 317, 630
- Landau, L. D. & Lifshitz, E. M. 1980, *Statistical physics. Pt.1, Pt.2*
- Lokas, E. L. 2002, *MNRAS*, 333, 697
- Lynden-Bell, D. 1967, *MNRAS*, 136, 101
- Merritt, D. 1996, *AJ*, 111, 2462
- Miller, R. H. 1964, *ApJ*, 140, 250
- Oman, K. A., Navarro, J. F., Fattahi, A., et al. 2015, *MNRAS*, 452, 3650
- Portegies Zwart, S., McMillan, S., Harfst, S., et al. 2009, *New A*, 14, 369
- Power, C., Navarro, J. F., Jenkins, A., et al. 2003, *MNRAS*, 338, 14
- Springel, V. 2005, *MNRAS*, 364, 1105
- Springel, V., Yoshida, N., & White, S. D. M. 2001, *New A*, 6, 79
- Valluri, M. & Merritt, D. 2000, *Advanced Series in Astrophysics and Cosmology*, 10, 229
- van den Bosch, F. C. & Ogiya, G. 2018, *MNRAS*, 475, 4066
- van den Bosch, F. C., Ogiya, G., Hahn, O., & Burkert, A. 2018, *MNRAS*, 474, 3043
- van Elteren, A., Pelupessy, I., & Portegies Zwart, S. 2014, *Philosophical Transactions of the Royal Society of London Series A*, 372, 20130385
- Walker, M. G. & Peñarrubia, J. 2011, *ApJ*, 742, 20
- Zhan, H. 2006, *ApJ*, 639, 617

6. Acknowledgements

The work is supported by the Program 28 of the fundamental research of the Presidium of the Russian Academy of Sciences "Space: research of the fundamental processes and relations", subprogram II "Astrophysical objects as space laboratories". The study is supported by the Supercomputing Center of Lomonosov Moscow State University. The study is supported by the "GOV-ORUN" Supercomputer, the Bogoliubov Laboratory of Theoretical Physics and Laboratory of Information Technologies, Joint Institute for Nuclear Research, Dubna, Russia.

This research is supported by the Munich Institute for Astro- and Particle Physics (MIAPP) of the DFG cluster of excellence "Origin and Structure of the Universe".

References

- Athanassoula, E., Fady, E., Lambert, J. C., & Bosma, A. 2000, *MNRAS*, 314, 475
- Barnes, J. & Hut, P. 1986, *Nature*, 324, 446
- Baushev, A. N. 2014a, *ApJ*, 786, 65
- Baushev, A. N. 2014b, *A&A*, 569, A114
- Baushev, A. N. 2015, *Astroparticle Physics*, 62, 47
- Baushev, A. N. 2016, *J. Cosmology Astropart. Phys.*, 1, 018
- Baushev, A. N. & Barkov, M. V. 2018, *J. Cosmology Astropart. Phys.*, 2018, 034